THE JOURNAL OF BIOLOGICAL CHEMISTRY
Vol. 270, No. 19, Issue of May 12, pp. 11222–11229, 1995
Printed in U.S.A.


# Histidine Tagging Both Allows Convenient Single-step Purification of Bovine Rhodopsin and Exerts Ionic Strength-dependent Effects on Its Photochemistry*

(Received for publication, December 7, 1994, and in revised form, February 20, 1995)

**Jacques J. M. Janssen‡, Petra H. M. Bovee-Geurts, Maarten Merkx, and Willem J. DeGrip**

*From the Department of Biochemistry, Center of Eye Research, University of Nijmegen, 6500 HB Nijmegen, The Netherlands*

**For rapid single-step purification of recombinant rhodopsin, a baculovirus expression vector was constructed containing the bovine opsin coding sequence extended at the 3′-end by a short sequence encoding six histidine residues. Recombinant baculovirus-infected *Spodoptera frugiperda* cells produce bovine opsin carrying a C-terminal histidine tag (v-opshis$_{6x}$). The presence of this tag was confirmed by immunoblot analysis. Incubation with 11-*cis*-retinal produced a photosensitive pigment (v-Rhohis$_{6x}$) at a level of 15–20 pmol/10$^6$ cells. The histidine tag was exploited to purify v-Rhohis$_{6x}$ via immobilized metal affinity chromatography. Optimized immobilized metal affinity chromatography yielded a binding capacity of ≥35 nmol of v-Rhohis$_{6x}$ per ml of resin and purification factors up to 500. Best samples were at least 85% pure, with an average purity of 70% ($A_{280\ nm}/A_{500\ nm}$ = 2.5 ± 0.4, $n$ = 7). Remaining contamination was largely removed upon reconstitution into lipids, yielding rhodopsin proteoliposomes with a purity over 95%.**

**Spectral analysis of v-Rhohis$_{6x}$ showed a small but significant red shift (501 ± 1 nm) compared to wild type rhodopsin (498 ± 1 nm). The p$K_a$ of the Meta I ↔ Meta II equilibrium in v-Rhohis$_{6x}$ is down-shifted from 7.3 to 6.4 resulting in a significant shift at pH 6.5 toward the Meta I photointermediate. Both effects are reversed upon increasing the ionic strength. FT-IR analysis of the Rho → Meta II transition shows that the corresponding structural changes are identical in wild type and v-Rhohis$_{6x}$.**

Rhodopsin is the major component of the outer segments of the vertebrate rod photoreceptor cell. This visual pigment consists of an integral membrane protein to which a chromophore, 11-*cis*-retinal, is covalently linked via a protonated Schiff base. Rhodopsin triggers the conversion of photon energy (light) into a graded membrane potential. The absorption of a photon leads to a number of discrete conformational changes in the protein moiety of the pigment (sequel of photointermediates → photocascade), finally resulting in the exposure of G-protein binding sites at the cytoplasmic surface of the protein. In the past decade, research has focused on analyzing the relationship between the structure of the receptor and its functional properties. Heterologous expression of the protein in combination with site-specific mutagenesis has become an attractive way to study this relationship. Several expression systems capable of *in vitro* biosynthesis of opsin have been described (1–5). Expression levels in these systems are usually quite low compared to total cell protein (<0.5%) and even to total membrane protein. For most analyses, recombinant rhodopsin therefore has to be extensively purified. Several methods have been described for the purification of recombinant rhodopsin (1, 4, 6). These methods often have the disadvantage that the obtained samples are still contaminated to a various extent with proteins derived from the cells, used for recombinant protein production (4, 6). Quite pure preparations can be obtained using immunoaffinity chromatography (1). However, this approach is expensive (monoclonal antibody, peptides for elution), laborious (antibody production, purification, and coupling), and fairly inefficient (low column capacity, recovery only in the order of 50%). Hence, this procedure is not very suitable for production of larger amounts (1–10 mg of purified protein) required for structural studies (crystallization, FT-IR spectroscopy,[1] NMR spectroscopy).

The recombinant baculovirus-based expression system is an excellent system for the production of larger amounts of recombinant bovine rhodopsin (6, 7). Thus far, we have used concanavalin A-Sepharose affinity chromatography to purify rhodopsin produced in this system (6), which, combined with reconstitution into proteoliposomes, yields reasonably pure preparations (60–80%). However, it is quite inefficient. Because of contaminating viral glycoproteins, the column capacity for recombinant rhodopsin is small, and a laborious elution profile has to be applied. Here we report on an alternative approach, using a histidine tag engineered onto the C terminus of bovine opsin. Histidine tagging for purification of recombinant proteins by means of IMAC has been used for a number of proteins both in prokaryotic (8–10) and eukaryotic (11) expression systems, including recombinant baculovirus (12–14). None of these proteins, however, belonged to the superfamily of heptahelical G-protein-coupled membrane receptors of which rhodopsin is a member. Membrane proteins have to be solubilized with the help of specific detergents which may impair affinity techniques. Hence, we have evaluated IMAC for purification of recombinant rhodopsin. Here we will demonstrate that an adapted IMAC allows relatively simple, highly efficient single-

* This work was funded by Grant CT930467 in the European Union Biotechnology Program. The costs of publication of this article were defrayed in part by the payment of page charges. This article must therefore be hereby marked "*advertisement*" in accordance with 18 U.S.C. Section 1734 solely to indicate this fact.

‡ To whom correspondence and reprint requests should be addressed: University of Nijmegen, Dept. of Biochemistry, P. O. Box 9101, 6500 HB Nijmegen, The Netherlands. Tel.: 31-80-616-413; Fax: 31-80-540-525.

[1] The abbreviations used are: FT-IR, Fourier transform infrared; IMAC, immobilized metal affinity chromatography; v-Rho, wild-type regenerated opsin produced *in vitro* by recombinant baculovirus; v-Rhohis$_{6x}$, C-terminally histidine-tagged regenerated opsin produced *in vitro* by recombinant baculovirus; DoM, dodecyl-β-1-maltoside; PIPES, 1,4-piperazinediethanesulfonic acid; MES, 4-morpholineethanesulfonic acid; HEPPS, 4-(2-hydroxyethyl)-1-piperazinepropanesulfonic acid; ds, double-stranded; NTA, nitrilotriacetic acid; PAGE, polyacrylamide gel electrophoresis.

step purification of histidine-tagged rhodopsin with an excellent purification factor (≥500). The procedure we developed is directly applicable to other membrane (receptor) proteins. Interestingly, the C-terminally located histidine tag slightly influences spectral properties (3 nm red-shift) and photocascade (downshift of the p$K_a$ of the Meta I ↔ Meta II equilibrium) of rhodopsin, however, without perturbing the structural changes accompanying the photocascade. The effects are fully reversible at higher ionic strength and probably represent unexpected electrostatic effects on selected rhodopsin properties.

## EXPERIMENTAL PROCEDURES

*Materials*—Dodecyl-β-1-maltoside (DoM) and nonyl-β-1-glucoside were prepared as described previously (15). PIPES, HEPPS and MES buffers were purchased from Research Organics Inc., Trolox from Aldrich, and leupeptin from Sigma. AgCl windows were obtained from Fisher Scientific Co.

*Construction of the Histidine Tag Transfer Vector (pAcJAC2)*—A unique *Bam*HI restriction sequence was engineered in front of the stop codon at the 3′-end of the cDNA-encoding bovine opsin (16) using the Bio-Rad MutaGene kit (Bio-Rad) according to the manufacturer's instructions. This changed the original 3′-end coding sequence from 5′-caa gtg gcg cct gcc taa gccc-3′ to 5′-caa gtg gat cct gcc taa gccc-3′ (Fig. 1*B*). Into this *Bam*HI site we inserted a short synthetic dsDNA sequence with *Bam*HI overhangs using the two complementary oligonucleotides 5′-gatcctcaccatcaccatcaccactagt-3′ and 5′-gatcactagtggtgatggtgatggtgag-3′. The resulting transfer vector, designated pAcJAC2 (Fig. 1*A*), encodes bovine opsin carrying 6 histidines at the C terminus (Fig. 1*B*). The sequence was confirmed by dideoxysequencing. We used pAcJAC2 to generate a recombinant baculovirus as described previously (17).

*Regeneration and Purification of v-Rhohis$_{6x}$*—Baculovirus propagation, transfection, isolation of recombinant virus, and Sf9 insect cell culture are performed as described previously (17, 18). Viral infection was performed at a multiplicity of infection of 5. Cells were harvested 3 days post-infection by centrifugation (4,000 × *g*, 10 min, 4 °C). Regeneration of v-opshis$_{6x}$ into v-Rhohis$_{6x}$ was accomplished in total cellular membrane preparations. Briefly, cell pellets were resuspended in buffer A (6.5 mM PIPES, 10 mM EDTA, 5 mM dithioerythritol, and 100 ng/ml leupeptin, pH 6.5) at $10^8$ cells/ml and lysed upon homogenization (Potter-Elvehjem-tube). Homogenized cells were centrifuged (30,000 × *g*, 20 min, 4 °C), and the pellet was resuspended in buffer B (20 mM PIPES, 130 mM NaCl, 10 mM KCl, 3 mM $MgCl_2$, 2 mM $CaCl_2$, 0.1 mM EDTA, and 100 ng/ml leupeptin, pH 6.5). All subsequent manipulations were performed in a nitrogen atmosphere and under dim red light (Schott-Jena, RG 645 cut-off filter). Retina lipids were added in 100-fold molar excess over v-opshis$_{6x}$, followed by 11-*cis*-retinal in a small volume of dimethylformamide (10-fold molar excess over v-opshis$_{6x}$) and solid dodecyl-β-1-maltoside (DoM) to 0.5 mM. Samples were rotated for 2 h at room temperature and centrifuged (30,000 × *g*, 20 min, 4 °C). v-Rhohis$_{6x}$ was solubilized from the pellet in the same buffer that was used to bind v-Rhohis$_{6x}$ to the $Ni^{2+}$ nitrilotriacetic acid agarose resin ($Ni^{2+}$-NTA; Qiagen). Several buffers were evaluated for the IMAC. Buffer C consisted of 20 mM HEPPS, 0.5 M NaCl, 0.1 mM phenylmethylsulfonyl fluoride, 100 ng/ml leupeptin, 1 mM imidazole, 50 μM Trolox, and 20 mM DoM (pH 8.0). Buffer D was identical with buffer C, except for 10 mM imidazole instead of 1 mM. Buffer E was identical with buffer C, except for buffer and pH: PIPES (pH 6.5) was used instead of HEPPS (8.0). The regenerated pellets were incubated with these buffers (1 ml/$10^8$ cells) for 2 h at room temperature to solubilize v-Rhohis$_{6x}$. Extracts were centrifuged (30,000 × *g*, 20 min, 4 °C) to remove insoluble material, and glycerol was added to a concentration of 15% (w/v). The solubilized v-Rhohis$_{6x}$ was then applied to the $Ni^{2+}$-NTA column at a flow rate of 1–2 ml/h for 16 h at 4 °C under continuous recycling. This flow rate was maintained throughout the entire procedure. Typically, we used a column volume of 1 ml for the v-Rhohis$_{6x}$ extract from 1–2 × $10^9$ infected insect cells. Unbound material was eluted from the column with the same buffer that was used for loading of the sample except that it was supplemented with 15% (w/v) glycerol and 20 mM nonylglycose instead of 20 mM DoM (10 column volumes). This was followed by a second rinse using the same buffer, but now containing 25 mM imidazole (4 volumes). The bound v-Rhohis$_{6x}$ was then eluted from the column using the same buffer (C, D, or E) supplemented with 100 mM imidazole and containing 20 mM nonylglucose instead of DoM and 130 mM instead of 500 mM NaCl (6 volumes).

*Reconstitution of Purified v-Rhohis$_{6x}$ into Retina Lipids*—Retina lipids were extracted from illuminated bovine retinae using standard procedures (19). The lipids were stored at −80 °C in the dichloromethane/methanol extract. Their concentration was determined by a modified Fiske-Subbarow phosphate assay (20). The aliquot required for reconstitution is dried with argon gas, dissolved in a small volume of methanol, and then diluted with buffer B containing 20 mM nonylglucose.

Purified v-Rhohis$_{6x}$ was concentrated to 3–10 nmol/ml on an Omega 30K filter (Filtron, Northborough, MA) and mixed with 1 volume of retina lipid extract (100-fold molar excess). This mixture was layered on top of a sucrose step gradient (10%, 20%, and 45% (w/w) in 3 × diluted buffer B) and spun overnight (100,000 × *g*, ≥16 h, 4 °C). Reconstituted v-Rhohis$_{6x}$ was collected from the 20% and/or 45% interface. Collected proteoliposomes were either diluted with the required buffer, and used for analysis, or with distilled water, pelleted (80,000 × *g*, 1 h, 4 °C), and stored at −80 °C until further use.

*Immunoblot Analysis*—Proteins were separated on a 12.5% SDS-polyacrylamide gel (21), transferred to nitrocellulose (Schleicher and Schull BA85, pore size 85), and probed with monoclonal or polyclonal antibodies (17). The anti-opsin antibodies Rho-1D4 (monoclonal) and CERNJS858 (polyclonal) have been described before (22, 23) and were used in 1:1000 dilution. The anti-histidine tag antiserum was obtained from Cappel, Organon Teknika N.V., Turnhout, Belgium and was also used 1:1000.

*UV/Vis Spectroscopy and Photolysis*—UV/Vis spectroscopy to determine absorbance band shape and $\lambda_{max}$ was routinely performed at pH 6.5 in buffer B supplemented with 20 mM DoM using a Perkin-Elmer λ15 recording spectrophotometer. Detergent was added to prevent light-scattering artifacts. The spectrum of detergent-solubilized samples was recorded, after addition of 1 M hydroxylamine to 50 mM, before and after illumination (5 min, 300-watt light bulb, KG1 heat filter, Schott, Mainz, FRG). For accurate determination of the $\lambda_{max}$, difference spectra were used (illuminated spectrum subtracted from the "dark" one).

The late photointermediates Meta I, Meta II, and Meta III were studied at 10 °C in proteoliposomes of v-Rhohis$_{6x}$, using isotonic solutions buffered with 20 mM PIPES (pH 6.5–7.0), 20 mM MES (pH 5.5–6.0), or 20 mM HEPPS (pH 7.5–9.5) (24). The photocascade was triggered by illumination for 15 s (Schott OG530 cut-off filter), and spectra were recorded every 3 minutes. After 30 min, hydroxylamine was added to 50 mM to convert all photoproducts into opsin and retinaloxime, and remaining rhodopsin was bleached away by a 5-min illumination.

*Fourier Transform Infrared (FT-IR) Difference Spectroscopy*—FT-IR spectra of the rhodopsin → Meta II transition were recorded in principle as described previously (25, 26). Briefly, 1 nmol samples were deposited on AgCl windows by isopotential spin-drying (27). The resulting films were hydrated with 3 μl of MES buffer (pH 5.5), covered with another AgCl window, sealed with Teflon tape, and mounted into a variable temperature cell (Specac P/N21500, Kent, UK). FT-IR spectra were recorded on a Mattson Cygnus 100 spectrometer (Madison, WI) equipped with a liquid nitrogen-cooled, narrow band MCT detector. Sample hydration was monitored by the ratio between the peak absorbance near 3400 $cm^{-1}$ (OH stretching mode of water) and near 2900 $cm^{-1}$ (CH stretching mode of protein and lipids). Rhodopsin → Meta II difference spectra were recorded at 10 °C. Spectra were taken at 8 $cm^{-1}$ resolution in 5-min blocks before and after illumination at (1280 scans/spectrum). Each sample was illuminated for 30 s in the spectrometer under computer control using a 12-V 20-watt halogen lamp equipped with Schott KG1 and OG530 cut-off filters. Difference spectra were computed by subtracting spectra before illumination from spectra taken after illumination, using the EXPERT-IR software (Mattson).

## RESULTS

*Construction of the Histidine Tag Transfer Vector pAcJAC2 and Generation of Recombinant Virus*—In order to introduce a tag consisting of six histidines at the C terminus of bovine opsin, the transfer vector pAcJAC2 was constructed (Fig. 1*A*). pAcJAC2 is derived from the baculovirus transfer vector pAcDZ1 (28). A short synthetic sequence encoding a histidine tag followed by a stop codon was introduced at the C terminus using two complementary oligonucleotides (Fig. 1*B*). As a result, the two alanine residues at the C terminus of opsin (Ala-346 and Ala-348) were substituted by an aspartic acid and the first histidine residue, respectively (Fig. 1*B*). These substitutions concern residues, which are not highly conserved. Also, the aspartic acid residue introduced should partly counterbalance the additional charge carried by the histidine tag.

A

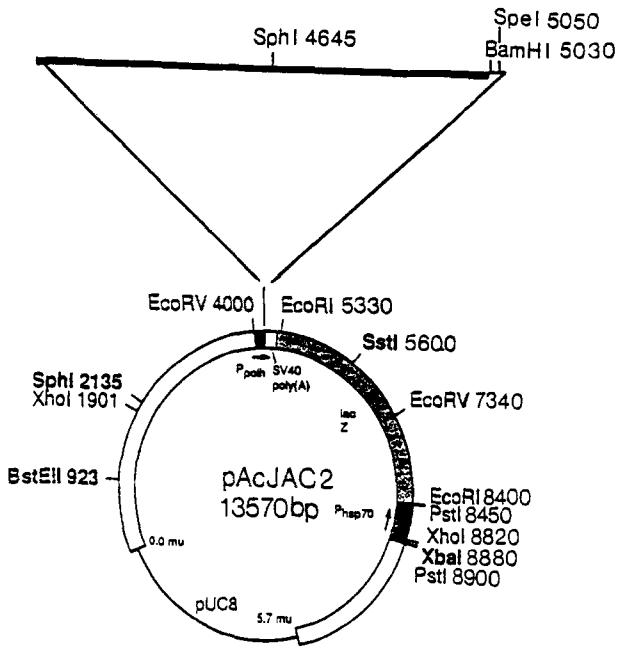


B

**Bovine opsin C-terminal sequence**

```
                                                                    1140
GAC GAC GAG GCC TCC ACC ACC GTC TCC AAG ACA GAG ACC AGC CAA GTG GCG CCT GCC TAA GCCCCAGGGACTCCGTGGC
Asp Asp Glu Ala Ser Thr Thr Val Ser Lys Thr Glu Thr Ser Gln Val Ala Pro Ala  .
                           340                                      348
```

**Bovine opsin containing a histidine-tag at the C-terminus**

```
                                                                    1140
GAC GAC GAG GCC TCC ACC ACC GTC TCC AAG ACA GAG ACC AGC CAA GTG GAT CCT CAC CAT CAC CAT CAC CAT TAG TGATC
Asp Asp Glu Ala Ser Thr Thr Val Ser Lys Thr Glu Thr Ser Gln Val Asp Pro His His His His His His
                           340                                      348
```

FIG. 1. **Cloning and C-terminal modification of v-opshis$_{6x}$.** *A*, schematic diagram of the transfer vector pAcJAC2. This vector was used to produce recombinant baculovirus AcNPV/opshis expressing bovine opsin carrying 6 histidine residues at the C terminus. The plasmid contains the cDNA encoding bovine opsin (▬). Opsin expression is controlled by the polyhedrin promoter ($P_{polh}$). The *Drosophila* hsp70 promoter ($P_{hsp70}$) and the *lacZ* marker gene, used to identify recombinant virus, are identical with vector pAcDZ1 (28). Cleavage sites for several restriction enzymes are denoted. *B*, the amino acid and DNA sequences of bovine opsin and the histidine-tagged opsin (designated v-opshis$_{6x}$) encoded by pAcJAC2, are displayed.

In pAcJAC2, opsin biosynthesis is controlled by the polyhedrin promoter while the small heat shock promoter of hsp70, drives the biosynthesis of β-galactosidase, which functions as a reporter enzyme (17, 28).

*Expression of v-opshis$_{6x}$ using Recombinant Virus AcNPV/opshis*—Protein samples derived from recombinant virus-infected Sf9 cells were analyzed by immunoblot, using a polyclonal antiserum elicited against bovine opsin (Fig. 2*A*). Wild-type virus-infected Sf9 cells are used as a negative control, and native bovine opsin and wild-type v-ops as positive controls (Fig. 2*A*, *lanes 1*, *2*, and *4*). The presence of the histidine tag in v-opshis$_{6x}$ was confirmed by the following observations: 1) only v-opshis$_{6x}$ is recognized by the histidine tag antibody (see below), 2) the apparent molecular mass of v-opshis$_{6x}$ is larger (by about 2 kDa) than that of native opsin and v-ops (Fig. 2*A*, *lane 3 versus lanes 2* and *4*), 3) v-opshis$_{6x}$ does not react with the monoclonal antibody 1D4 (Fig. 2*B*, *lane 1 versus 2*), since the C-terminal histidine tag extension eliminates the epitope for this antibody (29).

Hence, recombinant virus AcNPV/opshis directs expression of a fully intact histidine-tagged v-ops. The expression level varies between 20 and 30 pmol/$10^6$ cells, which is comparable to wild-type v-ops (6).

*Regeneration and Purification of v-Rhohis$_{6x}$*—To convert expressed v-opshis$_{6x}$ into v-Rhohis$_{6x}$, we incubated total membranes, harvested at 3 days post-infection from infected Sf9 cells, with 11-*cis*-retinal. Spectral analysis of regenerated samples showed that this resulted in 18 ± 2 pmol of v-Rhohis$_{6x}$ per $10^6$ cells ($n$ = 7). For purification by IMAC, regenerated samples were solubilized using DoM as a detergent and loaded onto

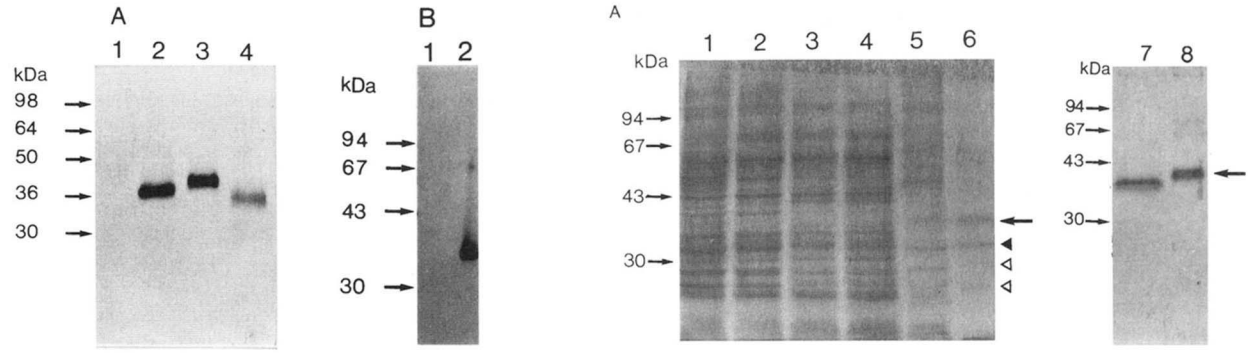


FIG. 2. **Immunoblot analysis of v-opshis$_{6x}$ expression.** Blots were screened with anti-rhodopsin antibodies: the polyclonal antiserums CERNJS858 (*A*) and the monoclonal, C-terminally directed Rho-1D4 (*B*), respectively. The *lanes* in *A* contain: mock-infected Sf9 cells (*lane 1*), native bovine opsin (*lane 2*), and Sf9 cells expressing v-opshis$_{6x}$ (*lane 3*) or v-ops (*lane 4*). *B*, native bovine opsin (*lane 2*) and v-opshis$_{6x}$ (*lane 1*). v-opshis$_{6x}$ clearly runs at higher apparent molecular mass than wild-type and is recognized by CERNJS858, but, in contrast to wild-type, not by 1D4.

a $Ni^{2+}$-NTA agarose column. This column appeared to bind v-Rhohis$_{6x}$ with high capacity. Proteins, which have natural affinity for metal ions are bound as well. A variety of washing and elution conditions have been tested to remove this contamination as much as possible without sacrificing binding capacity of the column and recovery of v-Rhohis$_{6x}$. Eluted fractions were analyzed by SDS-PAGE (protein pattern), immunoblotting (anti-rhodopsin CERNJS858 antiserum), and by UV/Vis spectroscopy ($A_{500}$ to detect and quantify v-Rhohis$_{6x}$; ratio $A_{280}/A_{500}$ as a purity indicator). Typical results are presented in Fig. 3 and Table I. *Lane 1* in Fig. 3, *A*, *B*, and *C*, presents the total extract of Sf9 membranes after regeneration. Only by immunoblot analysis can glycosylated v-opshis$_{6x}$ be identified (*arrow*) together with a minor amount of unglycosylated species (*arrowhead*). The nonbound, flow-through fraction shows a very similar protein pattern (*lane 2*), except that most v-Rhohis$_{6x}$ has bound, since only minimal amounts of the glycosylated form are detected in this fraction. Additional washings with extraction buffer (buffer C) elute a complex protein population (Fig. 3, *lanes 3* and *4*), probably representing aspecifically or very weakly bound proteins. The nonglycosylated v-opshis$_{6x}$ is already strongly present in these fractions (Fig. 3, *B* and *C*, *lanes 2–4*, *arrowhead*) and apparently is not very well retained by the column. Protein contamination, weakly interacting with the column, could be eluted by raising the imidazole concentration to 25 mM (Fig. 3, *lane 5*). Under these conditions, a minor amount of v-Rhohis$_{6x}$ was eluted. Most of the specifically bound v-Rhohis$_{6x}$, however, only was eluted upon raising the imidazole concentration to 100 mM (Fig. 3, *lane 6*). This fraction also contains a minor amount of nonglycosylated species and is still contaminated by several other minor bands (Fig. 3*A*, *lane 6*, *open arrowheads*).

The amount of nonglycosylated v-opshis$_{6x}$ in the DoM extract and column fractions varied between different experiments, but it was always present at immunodetectable levels (data not shown). In addition, immunoblots showed the presence of a third opsin species (Fig. 3*B*, *lanes 1–4*) which on SDS-PAGE gels migrated between the glycosylated and nonglycosylated v-opshis$_{6x}$. This species did not react with the anti-histidine tag antibody (Fig. 3*C*, *lanes 1–4*). We were unable to detect this band in the final purified v-Rhohis$_{6x}$ fraction (Fig. 3*B*, *lane 6*).

An overview of IMAC results obtained under two conditions, as determined by spectroscopic analysis, is given in Table I. Nearly complete binding of v-Rhohis$_{6x}$ to the $Ni^{2+}$-NTA agarose was attained. At pH 8.0 (buffer C), a pH at which IMAC is usually performed, an average recovery of 84% was achieved with a purification factor of at least 450. An attempt to reduce contamination by weakly binding proteins, by applying the membrane extract in the presence of a higher imidazole concentration (10 mM; buffer D), resulted in a much higher loss of v-Rhohis$_{6x}$ and in fact lowered the purification factor (not shown). Finally, the performance of the procedure we developed at pH 8.0, was evaluated at pH 6.5, since rhodopsin and most of its mutants are thermally much more stable at the

FIG. 3. **Typical purification profile of v-Rhohis$_{6x}$ using IMAC.** Fractions were analyzed by SDS-PAGE (*A*, Coomassie blue staining) and immunoblot (*B* and *C*). Immunoblots were screened with the polyclonal anti-rhodopsin antibody CERNJS858 (*B*) and the anti-histidine tag antibody (*C*). *Lane 1* represents the Sf9-cell membrane extract loaded onto the $Ni^{2+}$-NTA-agarose column. The nonbound fraction is shown in *lane 2*. *Lanes 3* and *4* represent early fractions eluted upon washing with buffer C, whereas *lane 5* contains the proteins that eluted from the column after supplementing buffer C with 25 mM imidazole. The strongly bound fraction, eluted from the column using buffer C supplemented with 100 mM imidazole, is shown in *lane 6*. *Lanes 7* and *8* in *A* represent purified, reconstituted native bovine rhodopsin (*lane 7*) and v-Rhohis$_{6x}$ (*lane 8*). Position of glycosylated (*large arrow*) and nonglycosylated (*small*, *filled arrowhead*) v-Rhohis$_{6x}$, as well as the intermediate de-histidine-tagged form (*large arrowhead*) and some minor contaminants in the purified fraction (*small open arrowheads*) are indicated. The immunopositive bands (*B* and *C*) and the Coomassie-positive band (*A*, *lane 8*) around 67 kDa represent a dimer of v-Rhohis$_{6x}$.

TABLE I
*General characteristics of v-Rhohis$_{6x}$ purification by IMAC as determined by UV/Vis spectroscopy*

Values given are mean ± S.D. of three experiments. The percentage solubilization is related to the amount solubilized under standard conditions (6), which was taken as the 100% value.

| | Condition | |
|---|---|---|
| | Buffer C | Buffer E |
| Solubization (%) | 100 ± 20 | 100 ± 8 |
| Nonbound (%) | 8 ± 5 | 5 ± 6 |
| Recovery (%) | 84 ± 4 | 80 ± 5 |
| $A_{280}/A_{500}$ | 2.7 ± 0.4 | 2.4 ±0.4 |

latter pH. This actually improved the purification factor to at least 500, without significant reduction in recovery (Table I, buffer E). At pH 6.5, best v-Rhohis$_{6x}$ samples had a purity of 80–85% ($A_{280}/A_{500}$ ratio of 2.0–2.1), and the average purity of combined fractions was 70–75%. The maximal capacity of the $Ni^{2+}$-NTA agarose column for v-Rhohis$_{6x}$ has not been determined exactly but is at least 35 nmol/ml bed volume. The efficiency of this IMAC procedure is spectrally illustrated in Fig. 4*A*. *Curve 1* represents the total membrane extract applied to the column, while *curve 2* presents the spectrum of the combined purified v-Rhohis$_{6x}$ fractions.

The contamination in the v-Rhohis$_{6x}$ fraction obtained after IMAC resides in several minor bands. These are largely removed upon subsequent reconstitution of v-Rhohis$_{6x}$ into retina lipid proteoliposomes, which represent a more native-like environment, we routinely use to analyze functional properties of recombinant rhodopsin (6). To simplify reconstitution, the detergent used during regeneration (DoM) is exchanged during IMAC for nonylglucose, which is more easily exchanged for phospholipids (30). The resulting v-Rhohis$_{6x}$ proteoliposomes contain at least 95% rhodopsin on a protein base and are suitable for all functional analyses (Fig. 3*A*, *lane 8*)

*Spectral Properties and Photocascade of v-Rhohis$_{6x}$—Curve 2* in Fig. 4*A* is a typical absorbance spectrum of the combined v-Rhohis$_{6x}$ fractions obtained after IMAC purification. Illumination of v-Rhohis$_{6x}$ "bleaches" the main absorbance band at 500 nm, and we used difference spectra to calculate the $\lambda_{max}$ more accurately. Unexpectedly, the absorbance band of v-Rhohis$_{6x}$ turns out to be slightly red-shifted ($\lambda_{max}$ = 501 ± 1 nm, $n$ = 7) relative to wild-type ($\lambda_{max}$ = 498 ± 1 nm) (Fig. 4*B*). This slight but significant red shift has been observed in all samples produced so far, both before and after IMAC purification. The shift is independent of the presence of 10 mM $Ni^{2+}$ ions (complexed histidine tag) or 10 mM EDTA (free histidine tag).

Analysis of the later part of the photocascade of reconstituted v-Rhohis$_{6x}$ presents another subtle effect of histidine tagging: at pH 6.5, the Meta I ↔ Meta II equilibrium is clearly shifted toward Meta I (Fig. 5*B*) in comparison to wild-type rhodopsin (Fig. 5*A*). At pH 5.5, v-Rhohis$_{6x}$ again behaves similar to wild-type (Fig. 5*C*: little Meta I formed, normal formation of Meta III). Again, this effect is not influenced by excess $Ni^{2+}$ ions or complexing agent (EDTA). Analysis over a larger pH range, in fact, demonstrates that the p$K_a$ of the Meta ↔ Meta II equilibrium is down-shifted about 1 pH unit from 7.3 in wild-type to 6.4 (Fig. 6).

Hence, we reasoned that these subtle changes in v-Rhohis properties might be due to the additional surface charge introduced by the histidine tag. Increasing the ionic strength by addition of KCl up to 1 M concentration indeed reverted $\lambda_{max}$ and photocascade of v-Rhohis$_{6x}$ to wild-type behavior (Table II).

*Structural Analysis of the Rho → Meta II Transition by FT-IR Spectroscopy*—FT-IR difference spectroscopy provides detailed structural information on the transitions in the rhodopsin photocascade (*e.g.* Refs. 25–27, 31, and 32). We have used this approach to investigate whether histidine tagging would also exert influence on the conformational changes accompanying Meta II formation. Comparison of the FT-IR difference spectra for the rhodopsin to Meta II transition in native rhodopsin and v-Rhohis$_{6x}$ shows that these spectra are highly similar (Fig. 7). All major bands characteristic of the formation of Meta II (numbers in $cm^{-1}$) are present in v-Rhohis$_{6x}$ as well and within experimental error (±2 $cm^{-1}$) at the same frequency as wild-type. Hence, the histidine tag does not detectably influence the conformational changes accompanying photoexcitation of rhodopsin.

## DISCUSSION

*Purification of Recombinant Membrane Receptors*—G-protein-coupled membrane receptor proteins have been expressed in all common *in vitro* expression systems (mammalian cell lines, insect cell lines, yeast, *Escherichia coli*), but the levels of expression are always low (<0.5% of cellular protein). Hence, for more elaborate functional studies as well as for structural studies, a very efficient purification procedure is needed. The most selective and frequently used approach is to exploit receptor affinity for an (ant)agonist or a monoclonal antibody. For instance, the most popular way to purify recombinant rhodopsins is by immunoaffinity chromatography over immobilized 1D4 (1, 33).

However, this approach has several disadvantages: it suffers from rather low recoveries (≤50% in our hands), low column capacity (1–2 nmol/ml bed volume), and expensive exploitation (monoclonal antibodies, peptide for elution). It is therefore not very suitable to purify larger amounts of recombinant protein. As an alternative, we adapted lectin affinity chromatography over concanavalin A-Sepharose to the recombinant baculovirus system (6, 17). This technique gives good recoveries (≥80%) and is fairly inexpensive, but due to the large contamination with viral glycoproteins, a complex elution profile has to be applied and the column capacity for rhodopsin binding is low (approximately 1 nmol/ml bed volume). As a consequence, it only affords rather low purification factors (50–100) and is quite laborious in the case of larger batches. We therefore searched for other alternatives and IMAC in combination with histidine tagging looked like a good candidate (8–13).

*IMAC Purification of Histidine-tagged Rhodopsin*—We selected the C-terminal of rhodopsin as a suitable site for appending a 6x histidine tag since 1) this site allows immunoaffinity purification and therefore should be well accessible and 2) C-terminal extension does not significantly influence functional properties of the protein (33, 34).[2]

Recombinant histidine-tagged bovine opsin could be successfully, functionally expressed in the recombinant baculovirus/insect cell expression system. Regeneration with 11-*cis*-retinal resulted in a pigment (v-Rhohis$_{6x}$) that could be purified almost to homogeneity in a single step using IMAC under optimized conditions. This purification procedure is rapid, fairly inexpensive, yields good recoveries (≥80%) with an excellent purification factor (≥500), and can handle, thanks to the high column capacity (≥35 nmol/ml bed volume), relatively large batches of rhodopsin. Interestingly, the histidine tag at the C terminus was found to have a subtle influence on the spectral and photolytic properties of this visual pigment, but these effects could be reversed by increasing the ionic strength.

The presence of the histidine tag at the C terminus of bovine opsin was first confirmed by immunoblot analysis. The modified C terminus was no longer recognized by the monoclonal antibody Rho-1D4 (29), and v-opshis$_{6x}$ was clearly identified by a polyclonal antibody elicited against a hexahistidine peptide.

[2] G. L. J. De Caluwé and W. J. De Grip, unpublished data.

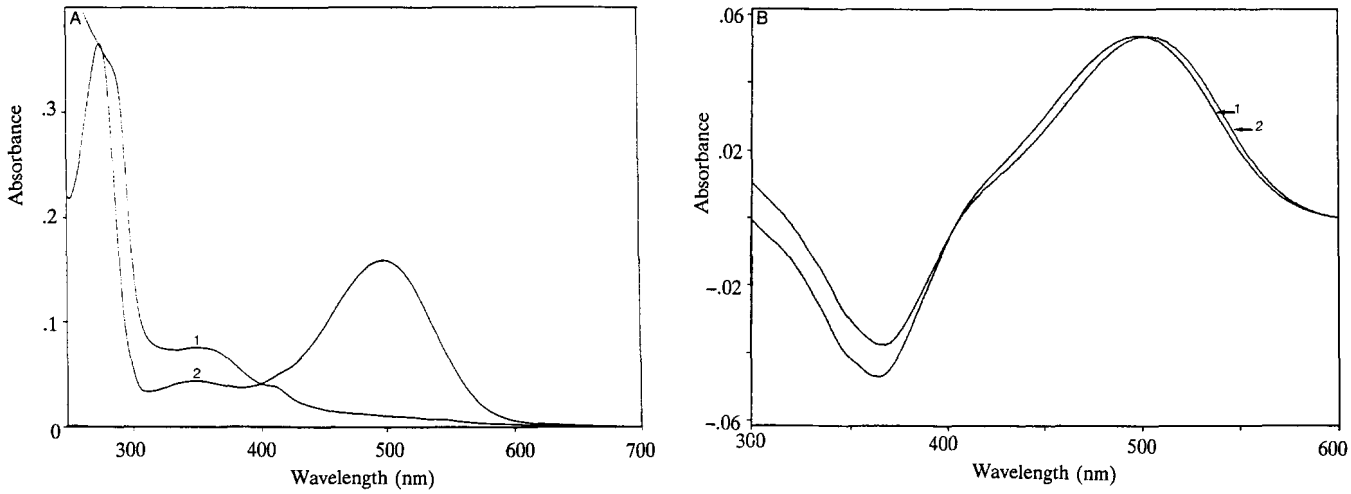


FIG. 4. **Spectral analysis of the IMAC purification of histidine-tagged rhodopsin.** *A*, UV/Vis absorbance spectrum of the regenerated DoM extract that was applied to the $Ni^{2+}$-NTA agarose column (*curve 1*); typical absorbance spectrum of v-Rhohis$_{6x}$ after purification by IMAC (*curve 2*). The two spectra were normalized to the absorbance at 278 nm, the maximum of the protein absorbance band. *B*, difference spectra (illuminated subtracted from dark) of purified v-Rho (*curve 1*) and v-Rhohis$_{6x}$ (*curve 2*). Spectra were recorded in the presence of 50 mM hydroxylamine.

In addition, the apparent molecular mass of v-opshis$_{6x}$ on the immunoblots has increased relative to v-ops. Our histidine tag should increase the molecular mass by approximately 0.7 kDa. The observed shift of the apparent molecular mass, seen on the immunoblots, is at least 2 kDa, however. This might reflect a direct or indirect (SDS binding) effect due to the additional charge introduced by the histidine residues, which would change the migration behavior on the gel. Such a large effect has not been reported before but it might be more pronounced in the case of membrane proteins, which by themselves usually show aberrant behavior in SDS-PAGE.

Ultimate proof for the presence of the histidine tag in v-opshis$_{6x}$ of course lies in the successful application of IMAC using $Ni^{2+}$ chelation. With this technique we could combine a high column capacity with high purification factors and good recoveries. The $A_{280}/A_{500}$ ratio indicates that, under optimized conditions, the combined purified fractions on average contain at least 70% v-Rhohis$_{6x}$. However, peak column fractions have been obtained in which this was as high as 80–85%. Immunoblot analysis shows that the purified v-Rhohis$_{6x}$ samples contain some nonglycosylated v-opshis$_{6x}$. Lack of glycosylation was reported to reflect impaired protein folding and loss of regeneration capacity (17, 35). Therefore, one of the contaminants present in the v-Rhohis$_{6x}$ samples is v-opshis$_{6x}$. Protein staining of PAGE gels reveals in addition to nonglycosylated v-opshis$_{6x}$ two minor bands at ca 25–30 kDa. Hence, these three proteins are the major contaminants after IMAC. Upon subsequent reconstitution into proteoliposomes, this remaining contamination is also largely removed. In the case of opsin this is due to its relative low stability in detergents and tendency to aggregate, which impairs correct reconstitution into a lipid matrix. Indeed, absolute FT-IR absorption spectra, where the amide I (1620–1690 $cm^{-1}$) and amide II (1530–1560 $cm^{-1}$) bands are extremely sensitive to protein secondary structure (36), do not suggest the presence of any (partially) misfolded opsin,[3] while this was clearly observed for the mutants E134D and E134R (31).

In addition to glycosylated and nonglycosylated (rhod)opsin, a third anti-opsin immunoreactive band was detected, primarily in the IMAC wash fractions. The latter band migrates between the first two bands and is not recognized by the anti-histidine tag antibodies. This opsin species is only formed in minor amounts (<5% of total), and, presently, it is not clear where it derives from. It could be due to chemical cleavage of the histidine tag on the column, *e.g.* in the $Ni^{2+}$-complexed from, or derive from endogenous carboxypeptidase activity present in the Sf9 cells. Both reactions might remove up to the entire tag, which would explain why this species has no or only low affinity for the $Ni^{2+}$-NTA agarose and is not recognized by the anti-histidine tag antibodies. Thus far, no one has described a similar observation or any carboxypeptidase activity in Sf9 cells although a C-terminal histidine-tagged protein has been purified from this expression system before (13). However, we only did observe this (partial) removal of the histidine tag from v-Rhohis$_{6x}$ because of the relative large difference in apparent molecular mass between v-Rho and v-Rhohis$_{6x}$ and the availability of the anti-histidine tag antiserum. In the earlier reports, no large difference in molecular mass between the native and histidine-tagged proteins was observed, and no antiserum against the histidine tag was available. On the other hand, carboxypeptidase activity has been previously put to good use to remove a polyhistidine peptide fused to dihydrofolate reductase after purification from expression in *E. coli* (9). Hence, if cleavage of the histidine tag does become a serious problem for certain proteins, it is recommendable either to include carboxypeptidase inhibitors during extraction and purification or to protect the histidine tag with a C-terminal proline residue or to insert/append it elsewhere into the protein.

*Functional Properties of v-Rhohis$_{6x}$*—The expressed v-opshis$_{6x}$ smoothly recombines with the chromophore, 11-*cis*-retinal, into a functional photopigment. However, unexpectedly, the absorbance spectrum of v-Rhohis$_{6x}$ shows a small but significant red shift ($\lambda_{max}$ = 501 nm) and the p$K_a$ of the Meta I ↔ Meta II equilibrium is shifted down. These effects are not due to the presence of a $Ni^{2+}$-histidine tag complex, since they do not depend on the presence of $Ni^{2+}$ ions and are not reversed by addition of an excess of the complexing agent EDTA. However, both shifts are fully reversed by the addition of 1 M KCl. Hence, presently we think that these subtle functional effects result from the additional surface charge introduced by the histidine tag at the cytoplasmic surface of v-Rhohis$_{6x}$. This could lead to an alkaline shift in the surface pH, which could explain the apparent downshift of the p$K_a$ of the Meta I ↔ Meta

[3] J. J. M. Janssen, P. H. M. Bovee-Geurts, M. Merkx, and W. J. DeGrip, unpublished observations.

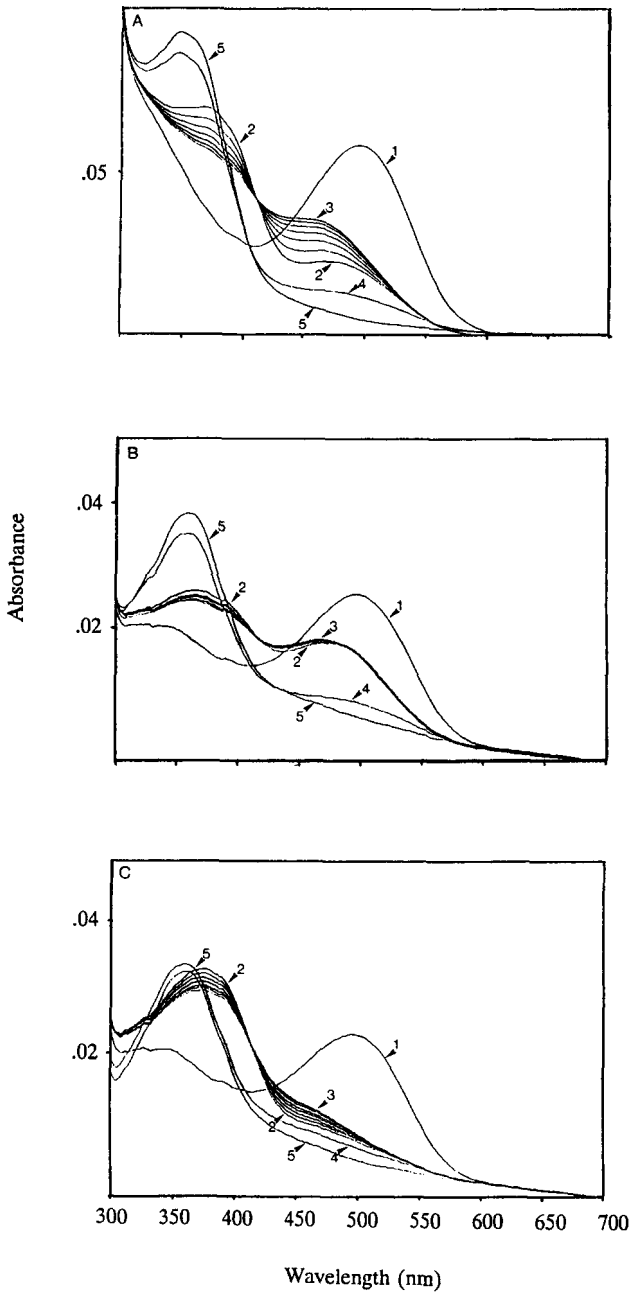


FIG. 5. **Spectral analysis of late photointermediates (Meta I, Meta II, and Meta III).** v-Rho (*A*) and v-Rhohis$_{6x}$ (*B* and *C*) were reconstituted in retina lipid proteoliposomes. Spectra shown in *A* and *B* were recorded at pH 6.5. The spectrum shown in *C* was obtained at pH 5.5. Upon illumination, the dark spectrum (*spectrum 1*) is converted into an equilibrium mixture of Meta II (380 nm) and Meta I (480 nm) (*spectrum 2*), which slowly decays under formation of Meta III (level after 30 min; *spectrum 3*). Addition of hydroxylamine then converts all photoproducts into opsin, retinaloxime, and remaining rhodopsin (*spectrum 4*). A final illumination bleaches away remaining rhodopsin (*spectrum 5*).

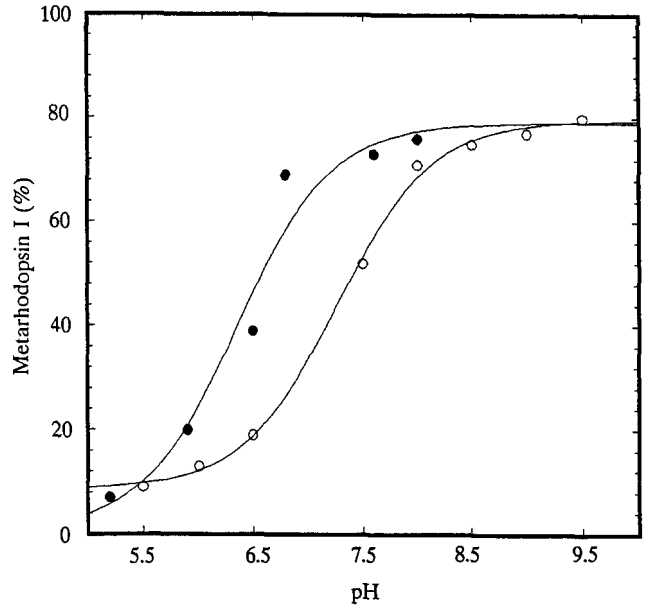


FIG. 6. **pH dependence of the Meta I ↔ Meta II equilibrium of v-Rho and v-Rhohis$_{6x}$.** Percentage of Meta I present upon illumination of reconstituted v-Rho (*open circles*) or v-Rhohis$_{6x}$ (*closed circles*) was measured in dependence of pH. Data points were fitted with the Henderson-Hasselbach equation for a single group titration, yielding a p$K_a$ of 7.3 for v-Rho and 6.4 for v-Rhohis$_{6x}$.

TABLE II

*Reversal of histidine tag effects by an increase in ionic strength*

The $\lambda_{max}$ was determined from difference spectra (*cf.* Fig. 4*B*). The percentage of Meta I remaining in the Meta I ↔ Meta II photoequilibrium at pH 6.5 is calculated from the absorbance difference at 480 nm (spectrum 2 minus 4 in Fig. 5). Mean ± S.D. of *n* determinations is given. This increase in ionic strength does not significantly affect this proportion in bovine rhodopsin.

| | KCl | $\lambda_{max}$ | Meta I remaining |
|---|---|---|---|
| v-Rhohis$_{6x}$ | 0.1 | 501 ± 1 ($n$ = 7) | 44 ± 5 ($n$ = 4) |
| | 1.1 | 499 ± 1 ($n$ = 2) | 15 ± 3 ($n$ = 2) |
| v-Rho | 0.1 | 498 ± 1 ($n$ = 15) | 19 ± 4 ($n$ = 5) |

II equilibrium. In addition, electrostatic effects (either local or more general like an increase in the protein dipole) could be involved. Both effects would indeed be suppressed by an increase in ionic strength. It would be quite exciting if electrostatic effects could at least partially be responsible for the observed phenomena, since to our knowledge such "long range influence" has not been documented yet. We are presently investigating this in more detail by mapping bulk-pH dependence, measuring surface pH, establishing reversal by removal of the histidine tag, and insertion of the histidine tag in other positions.

In order to establish whether the effect of the histidine tag would also penetrate at the structural level, FT-IR analysis was performed. The band shape of the amide I band indicates a very similar secondary structure composition for rhodopsin and v-Rhohis$_{6x}$, and the FT-IR difference spectra corresponding to the rhodopsin to Meta II transition are also highly similar. All characteristic bands of this transition (at 970, 1552, 1643, 1686, 1712, 1728, 1750, and 1768 cm$^{-1}$; the latter two of which have recently been assigned to the C=O stretching mode of aspartic acid 83 (31, 32)) are also present in the difference spectrum obtained with v-Rhohis$_{6x}$. Hence, according to analysis by FT-IR, no significant differences exist in the structural alterations accompanying receptor activation in rhodopsin or v-Rhohis$_{6x}$.

*Conclusion*—The use of IMAC in combination with histidine tagging has considerably improved and simplified the purification of recombinant rhodopsin. This will now permit us to further scale up the cell culture volume and recombinant protein production, which thereby will yield sufficient protein for more detailed structural studies, requiring modified protein (FT-IR, NMR, crystallization).

The adaptations we have introduced in the IMAC (use and exchange of detergents, lower pH, stepwise imidazole elution) should make it applicable for membrane proteins in general. It cannot be foreseen whether the subtle influence of the histidine

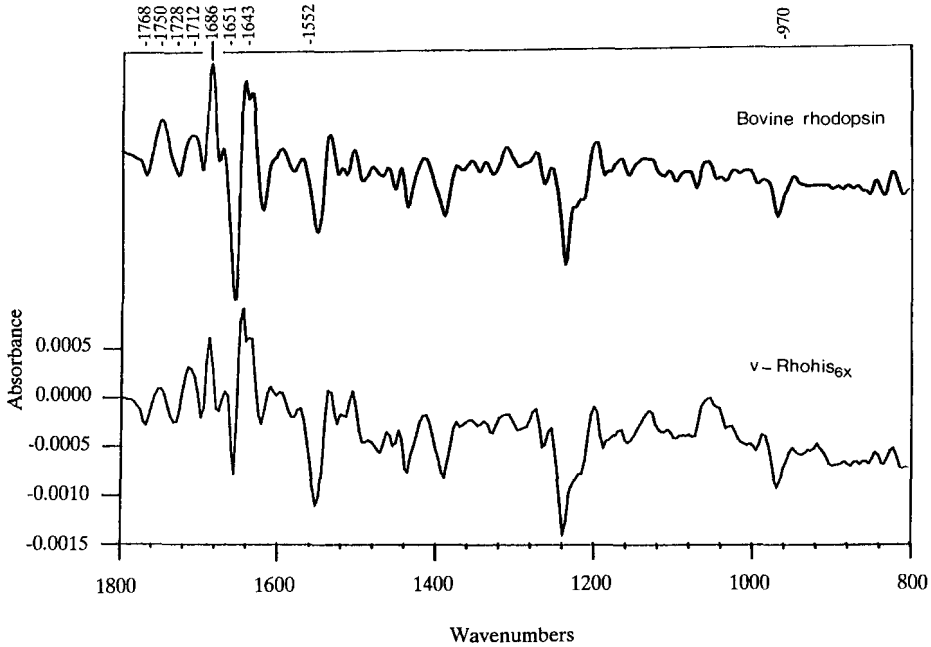


FIG. 7. **FT-IR analysis of photoexcitation.** FT-IR difference spectra are presented corresponding to the Rho → Meta II transition of reconstituted native bovine rhodopsin (*upper spectrum*) or v-Rhohis$_{6x}$ (*lower spectrum*). Both transitions were recorded at 10 °C and pH 5.5 at isotonic ionic strength. Bands characteristic for Meta II formation are indicated by *wavenumber* (cm$^{-1}$).

tag on functional properties, observed for rhodopsin, would also always emerge in other membrane receptors. However, the histidine tag apparently need not influence the conformational changes accompanying receptor activation, and any functional effects can easily be suppressed by an increase in ionic strength or, if properly placed, be abolished by its proteolytic removal.

*Acknowledgments*—We are grateful to Dr. Robert S. Molday (University of British Colombia, Vancouver, Canada) for providing the hybridoma producing 1D4 and to Dr. Just M. Vlak and Dr. Douwe Zuidema (University of Wageningen, The Netherlands) for making available the transfer vector pAcDZ1.

REFERENCES

1. Oprian, D. D., Molday, R. S., Kaufman, R. J., and Khorana, H. G. (1987) *Proc. Natl. Acad. Sci. U. S. A.* **84,** 8874–8878
2. Janssen, J. J. M., VanDeVen, W. J. M., VanGroningen-Luyben, W. A. H. M., Roosien, J., Vlak, J. M., and DeGrip, W. J. (1988) *Mol. Biol. Rep.* **13,** 65–71
3. Khorana, H. G., Knox, B. E., Nasi, E., Swanson, R., and Thompson, D. A. (1988) *Proc. Natl. Acad. Sci. U. S. A.* **85,** 7917–7921
4. Nathans, J., Weitz, C. J., Agarwal, N., Nir, I., and Papermaster, D. S. (1989) *Vision Res.* **29,** 907–914
5. Zozulya, S. A., Gurevich, V. V., Zvyaga, T. A., Shirokova, E. P., Dumler, I. L., Garnovskaya, M. N., Natochin, M. Y., Shmukler, B. E., and Badalov, P. R. (1990) *Protein Eng.* **3,** 453–458
6. DeCaluwé, G. L. J., VanOostrum, J., Janssen, J. J. M., and DeGrip, W. J. (1993) *Methods Neurosci.* **15,** 307–321
7. Janssen, J. J. M., DeCaluwé, G. L. J., and DeGrip, W. J. (1990) *FEBS Lett.* **260,** 113–118
8. Gentz, R., Certa, U., Takaes, B., Matile, H., Döbeli, H., Pink, R., Mackay, M., Bone, N., and Scafi, J. G. (1988) *EMBO J.* **7,** 225–230
9. Hochuli, E., Bannwarth, W., Döbeli, H., Gentz, R., and Stüber, D. (1988) *Bio/Technology* **6,** 1321–1325
10. Smith, M. C., Furman, T. C., Ingolia, T. D., and Pidgeon, C. (1988) *J. Biol. Chem.* **263,** 7211–7215
11. Janknecht, R., DeMartynoff, G., Lou, J., Hipskind, R. A., Nordheim, A., and Stunnenberg, H. G. (1991) *Proc. Natl. Acad. Sci. U. S. A.* **88,** 8972–8976
12. Chen, X., Brash, A. R., and Funk, C. D. (1993) *Eur. J. Biochem.* **214,** 845–852
13. Wang, M., Bentley, W. E., and Vakharia, V. (1994) *Biotechnol. Bioeng.* **43,** 349–356
14. Reddy, R. G., Yoshimoto, T., Yamamoto, S., Funk, C. D., and Marnett, L. J. (1994) *Arch. Biochem. Biophys.* **312,** 219–226
15. DeGrip, W. J., and Bovee-Geurts, P. H. M. (1979) *Chem. Phys. Lipids* **23,** 321–335
16. Nathans, J., and Hogness, D. S. (1983) *Cell* **34,** 807–814
17. Janssen, J. J. M., Mulder, W. R., DeCaluwé, G. L. J., Vlak, J. M., and DeGrip, W. J. (1991) *Biochim. Biophys. Acta* **1089,** 68–76
18. Summers, M. D. and Smith, G. E. (1987) *Texas Exp. Station Bull.* 1555
19. Hendriks, T., Klompmakers, A. A., Daemen, F. J. M., and Bonting, S. L. (1976) *Biochim. Biophys. Acta* **433,** 271–281
20. Broekhuyse, R. M. (1968) *Biochim. Biophys. Acta* **152,** 307–315
21. Laemmli, U. K. (1970) *Nature* **227,** 680–685
22. Molday, R. S., and MacKenzie, D. (1983) *Biochemistry* **22,** 653–660
23. DeGrip, W. J. (1985) *Progr. Retinal Res.* **4,** 137–180
24. Cotton, R. G. H. (1993) *Mutat. Res.* **285,** 125–144
25. Rothschild, K. J., Gillespie, J., and DeGrip, W. J. (1987) *Biophys. J.* **51,** 345–350
26. DeGrip, W. J., Gray, D., Gillespie, J., Bovee-Geurts, P. H. M., VanDenBerg, E., Lugtenburg, J., and Rothschild, K. J. (1988) *Photochem. Photobiol.* **48,** 497–504
27. DeGrip, W. J., Gillespie, J., and Rothschild, K. J. (1985) *Biochim. Biophys. Acta* **809,** 97–106
28. Zuidema, D., Schouten, A., Usmany, M., Maule, A. J., Belsham, G. J., Roosien, J., Klinge-Roode, E. C., VanLent, J. W. M., and Vlak, J. M. (1990) *J. Gen. Virol.* **71,** 2201–2209
29. Molday, R. S. (1989) *Progr. Retinal Res.* **8,** 173–209
30. DeGrip, W. J., Olive, J., and Bovee-Geurts, P. H. M. (1983) *Biochim. Biophys. Acta* **734,** 168–179
31. Rath, P., DeCaluwé, G. L. J., Bovee-Geurts, P. H. M., DeGrip, W. J., and Rothschild, K. J. (1993) *Biochemistry* **32,** 10277–10282
32. Fahmy, K., Jäger, F., Beck, M., Zvyaga, T. A., Sakmar, T. P., and Siebert, F. (1993) *Proc. Natl. Acad. Sci. U. S. A.* **90,** 10206–10210
33. Oprian, D. D., Asenjo, A. B., Lee, N., and Pelletier, S. L. (1991) *Biochemistry* **30,** 11367–11372
34. Borjigin, J., and Nathans, J. (1994) *J. Biol. Chem.* **269,** 14715–14722
35. Sung, C.-H., Schneider, B. G., Agarwal, N., Papermaster, D. S., and Nathans, J. (1991) *Proc. Natl. Acad. Sci. U. S. A.* **88,** 8840–8844
36. Rothschild, K. J., DeGrip, W. J., and Sanches, R. (1980) *Biochim. Biophys. Acta* **596,** 338–351

**Histidine tagging both allows convenient single-step purification of bovine rhodopsin and exerts ionic strength-dependent effects on its photochemistry**

JJ Janssen, PH Bovee-Geurts, M Merkx and WJ DeGrip

*J. Biol. Chem. 1995, 270:11222-11229.*
*doi: 10.1074/jbc.270.19.11222*